FISSION-FRAGMENT MASS-ASYMMETRY ACCOMPANYING NUCLEAR POINCARÉ SHAPE TRANSITIONS*

K. Mazurek[a], J. Dudek[b], A. Maj[a], M. Kmiecik[a]

[a]The Henryk Niewodniczański Institut of Nuclear Physics
Polish Academy of Sciences
Radzikowskiego 152, 31-342 Kraków, Poland
[b]IPHC/DRS and Université de Strasbourg
23 rue du Loess, B.P. 28, 67037 Strasbourg Cedex 2, France

(Received November 10, 2015)

Fission fragment mass- and charge-distributions are among those experimental observables which could be directly compared to the theoretical predictions related to the Poincaré shape transitions accompanying an increase of the nuclear angular momentum. We apply the macroscopic nuclear liquid drop model to illustrate some characteristic features of the Poincaré transitions focusing on the static and dynamical estimates of the fission fragment mass-asymmetry. As an example, the results for ^{98}Mo are shown.

DOI:10.5506/APhysPolBSupp.8.611
PACS numbers: 21.60.–n, 21.10.–k, 24.75.+, 25.70.Gh

1. Method

Shape transitions of gravitating objects such as stars and planets have been the subject of interest for philosophers, mathematicians and physicists over the centuries. An increase in the frequency of rotation of such astronomical bodies is accompanied by a change in their form from the spherical one, through oblate and tri-axial arriving at strongly elongated prolate shapes before they possibly fission, as described for the first time by Jacobi [1]. Later on, Poincaré continuing the study of rotating masses, found out that another form of the evolution may become possible: the rotating bodies may loose their original left–right symmetry and undergo what is today referred to as Poincaré transitions [2]. An experimental evidence of the Jacobi transition in rotating nuclei can be found in Refs. [3, 4], where the techniques

* Presented at the XXII Nuclear Physics Workshop "Marie and Pierre Curie", Kazimierz Dolny, Poland, September 22–27, 2015.

similar to the ones employed in this article have been used to describe the evolution of the strength function of the Giant Dipole Resonances (GDR) with increasing spin, as a function of the changing most probable nuclear shape.

Modeling of the high-temperature Poincaré shape transitions, possibly competing with the Jacobi ones, can conveniently be performed using the realistic modeling of the total nuclear energy — similar to the one in Ref. [5]. The first studies of this mechanism, *cf.* Refs. [6–8], allowed to choose the optimal sets of deformation parameters necessary to describe such an exotic phenomenon theoretically. A recent extension of the classical liquid drop model approach to include the dynamical, in particular the large amplitude motion effects in the context of the nuclear shape transitions can be found in Ref. [9].

In the present article, we consider nuclei at the high temperature limit. This allows us to employ the macroscopic liquid drop model alone to describe the energies and, as a consequence, the equilibrium and/or the most probable shapes of the rotating nuclei. Here, we use the so-called Lublin–Strasbourg Drop (LSD) model, *cf.* Refs. [5,10,11]. The nuclear shapes are parameterized in terms of the spherical harmonics $Y_{\lambda\mu}$

$$R(\vartheta,\varphi) = R_0 c(\alpha)\left[1 + \sum_{\lambda=2}^{\lambda_{\max}} \sum_{\mu=-\lambda}^{\lambda} \alpha^{\star}_{\lambda\mu} Y_{\lambda\mu}(\vartheta,\varphi)\right], \tag{1}$$

where $R(\vartheta,\varphi)$ represents the nuclear surface, and function $c(\alpha)$ assures the constant volume condition. In the following, we use either the two-dimensional axial-quadrupole axial-octupole projection-plane (α_{20}, α_{30}) or one-dimensional projections on the α_{30}-axis. The latter are obtained after minimizing the total energy over 12 deformation parameters (α_{22}, α_{40}, α_{50}, α_{60}, α_{70}, α_{80}, α_{90}, α_{100}, α_{110}, α_{120}). The algorithm assures that the center of mass remains at the origin of the coordinate frame and does not change when the odd-λ multipole-deformations vary.

The effects of the collective motion underlying the effects of the mass asymmetry will be described approximately using the one-dimensional sections of the total nuclear potential energies along the octupole deformation-axis. Indeed, this is α_{30}-deformation which characterizes the nuclear left–right asymmetry and describes, to a leading order, the nuclear Poincaré transitions. The corresponding one-dimensional collective Hamiltonian will be taken in the form of

$$\hat{H} = \frac{\hbar^2}{2B}\frac{d^2}{d\alpha_{30}^2} + V(\alpha_{30}), \tag{2}$$

where B is the effective mass parameter characterizing the collective inertia against the octupole type shape changes. It will be taken in the form of a constant; to assure the correct order of magnitude estimate, this parameter will be adjusted in such a way that the energy of the zero-point motion associated with the octupole collective motion and, in particular, the octupole vibrations is, by convention, equal to 1 MeV. Function $V(\alpha_{30})$ is the corresponding projection of the macroscopic potential energy onto the octupole axis.

The solutions of the Schrödinger equation allow to obtain the most probable dynamical deformation. We take as a measure of this quantity the associated r.m.s. value $\bar{\alpha}_{30}$, defined as follows:

$$\left\langle \alpha_{30}^2 \right\rangle = \int d\alpha \Psi_n^*(\alpha) \alpha_{30}^2 \Psi_n(\alpha) \rightarrow \bar{\alpha}_{30} = \sqrt{\left\langle \alpha_{30}^2 \right\rangle}\,. \tag{3}$$

The latter allows to obtain the associated dispersion of the form

$$\sigma_{30} \equiv \sqrt{\left\langle \alpha_{30}^2 \right\rangle - \left\langle \alpha_{30} \right\rangle^2}\,. \tag{4}$$

The discussion of the possible extension of the method to two-dimensional Hamiltonian is presented in [9].

2. Results

The potential energy landscapes shown in Fig. 1 for rotating ^{98}Mo nucleus illustrates the evolution of the static energy minima with spin. The static equilibrium shapes become more and more elongated with increasing angular momentum. At spins of about $68\,\hbar$, the left–right symmetry measured in terms of the static equilibrium deformations can be considered broken, even though at significantly lower spins there is a pronounced softness in terms of the octupole deformation.

In this article, we discuss, in particular, the mass and the charge distributions of the fission fragments produced in the process of fission of excited compound nuclei. Here, the results are illustrated on the example of the ^{98}Mo compound system, but similar procedure can be employed for any other nucleus of interest. The nuclear densities are obtained microscopically after diagonalisation of the deformed Woods–Saxon mean-field Hamiltonian, for protons and neutrons separately. Figure 2 shows the density of protons as a function of variable z (according to the shape parameterization used, the $\mathcal{O}_z$-axis is the nuclear symmetry axis).

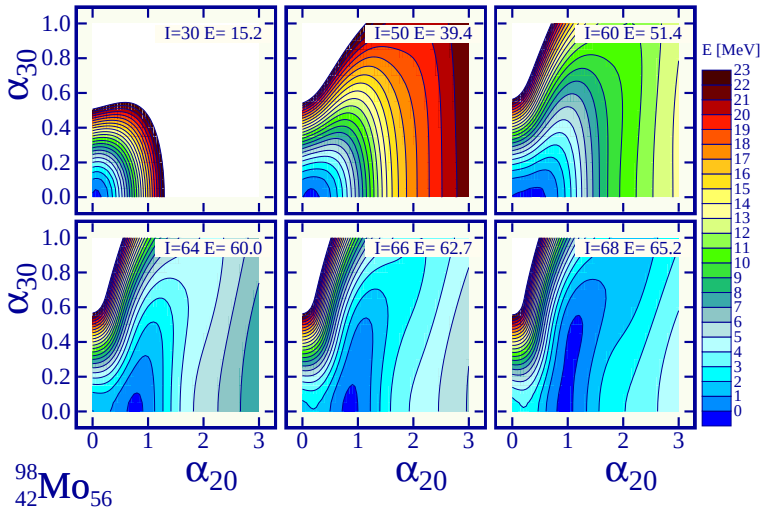

Fig. 1. The potential energy surfaces over the axial quadrupole and octupole deformation-plane for ^{98}Mo. The energy has been minimized over α_{22}, α_{40}, α_{50}, α_{60}, α_{70}, α_{80}, α_{90}, α_{100}, α_{110}, α_{120} deformations. The energies at the minima are expressed relative to the spherical energy minimum at zero spin; they are given in the boxes.

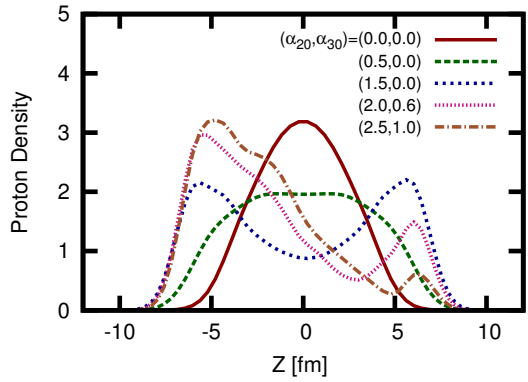

Fig. 2. Examples of the nuclear matter density profiles obtained with the help of the Woods–Saxon single particle Hamiltonian for a few sets of deformation parameters given in the field of the figure.

The nuclear density profiles follow the shape of the nucleus and are similar for protons and neutrons. The first and the second derivatives over z of the nuclear density profiles are shown for completeness (Fig. 3). Even though they may contain certain fluctuations which are of no particular significance for the present discussion, they are useful in the numerical algorithm.

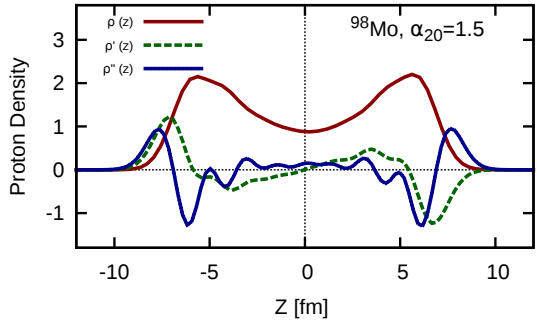

Fig. 3. Proton density profile and its derivatives for the shape of ^{98}Mo at spin 60 $\hbar$. The corresponding elongation is principally characterized by the quadrupole deformation, here $\alpha_{20} = 1.5$.

The calculated charge partition between the two fission fragments and the neck is presented in Fig. 4 (a) as a function of the elongation of the nucleus. The shapes for which the proton numbers displayed have been obtained were taken along the path to fission at the spin of 60 $\hbar$ for ^{98}Mo compound system. With an increasing elongation, the octupole deformation begins to play an important role, as it can be seen from Fig. 1. This is visible from Fig. 4 (a), in which the difference between the charges of the light and of the heavy fragments increases significantly for elongations in excess of $\alpha_{20} = 1.2$. The transition from symmetric and asymmetric shape is manifested by the temporary increasing number of nucleons in the neck.

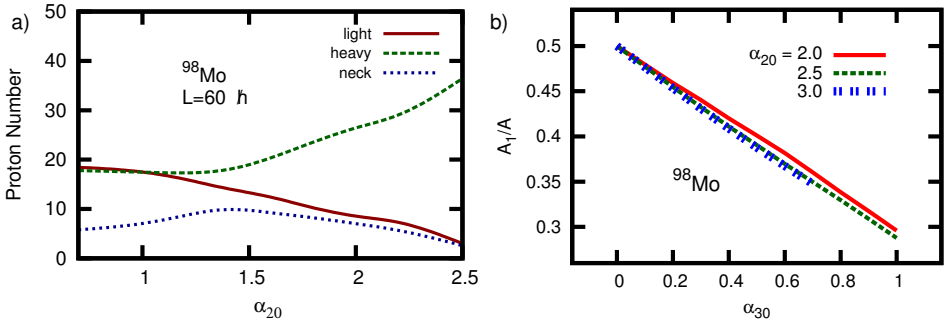

Fig. 4. (a) Evolution of the charge number in fission fragments and the nuclear neck along the path to fission. (b) Mass asymmetry of the light fission fragment (A_1/A) for three nuclear elongations: $\alpha_{20} = 2.0$, 2.5 and 3.0 for ^{98}Mo. (Minimization over $\alpha_{\lambda 0}$ for $\lambda \leq 12$.)

The minimum of energy for this system, at spin $60\,\hbar$, corresponds to $\alpha_{20} = 0.6$. The saddle point corresponds to $\alpha_{20} = 2.5$, the deformation very close to the scission deformation. Figure 4 (b) shows that the ratio A_1/A decreases almost linearly with the octupole deformation; this decrease is almost independent of the quadrupole α_{20} deformation.

The above discussion addresses the static nuclear deformation. It allows to connect the values of the octupole deformation with the number of protons and neutrons in the nascent fragments. In the present calculations, the deformations of protons and neutrons are kept the same, thus the shapes of the corresponding density functions are similar.

The effects of the dynamical deformation of the nucleus can be estimated using Eqs. (3)–(4). In particular, we may calculate in this way the most probable (expected) values of some measures of the nuclear shapes as *e.g.* the r.m.s. $\bar{\alpha}_{30}$-values.

As it can be deduced from Eq. (3) and can be seen from the example in Fig. 5, the dynamical octupole deformation of the nucleus is always different from zero. In the illustrated case, the dynamical octupole deformation increases significantly at the spins of about $60\,\hbar$ and the associated dispersion increases as well. This effect is related to the flattening of the potential energy landscapes visible in Fig. 1.

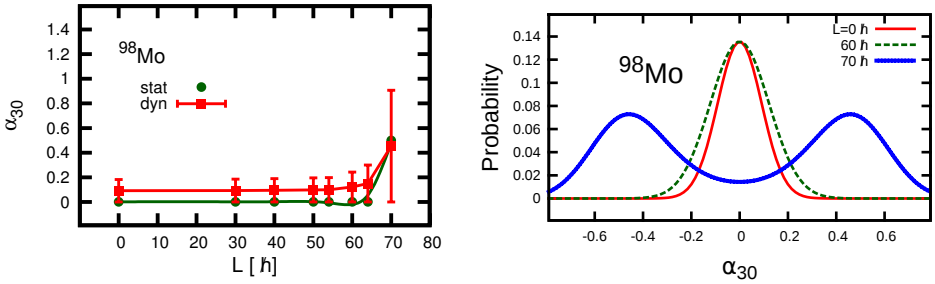

Fig. 5. (Color on-line) Left: The static octupole deformations (green circles) by definition correspond to the minima of the potential energy landscapes. The dynamical ones (red squares), $\bar{\alpha}_{30}$, are defined according to Eq. (3). Right: The probability density functions of the octupole shapes for spins displayed for the lowest energy (zero phonon) collective solutions.

Figures 5 (right) and 6 (right) show the probability density functions obtained with the help of the solutions of the collective Schrödinger equation, *cf.* Eq. (2). Since the mass asymmetry is directly associated with the octupole deformation the probability densities shown relate to this quantity. This information is essential in order to analyze correctly, *i.e.* in accordance with the quantum mechanical solutions of the Schrödinger equation of the collective motion, the experimental data which could confirm the presence

of the Poincaré transition. Changing of the nuclear shape from prolate to octupole-deformed with increasing angular momentum would be manifested in the experiment as a widening of the mass distribution of the fission fragments.

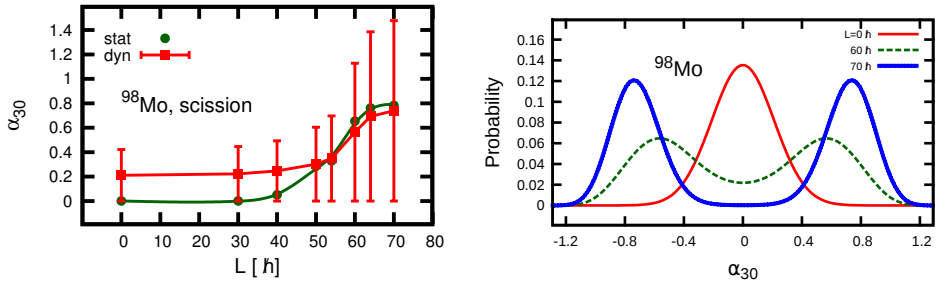

Fig. 6. (Color on-line) Similar to Fig. 5 but at elongations corresponding to scission.

3. Summary

The nuclear Poincaré transitions take place during the shape evolution of the nucleus with increasing spin, if the originally present left–right symmetry is lost at certain critical spin value. This breaking of the left–right symmetry results in an increase of the charge and mass asymmetry of the fission fragments.

The corresponding observables, such as predicted evolution of the charge of the light and heavy fission fragments and the probability of the mass asymmetry for chosen spins, have been calculated in this article and illustrated at an example of the nucleus ^{98}Mo. The experimental evidence of the Poincaré transition is expected to be manifested first of all by the widening of the fission fragment mass/charge distributions with increasing spin. The experimental data concerning the mass distribution of the fission fragments of hot medium mass nuclei as a function of increasing/decreasing spin are necessary for further advancements in this field.

This work has been partly supported by the National Science Centre under Contract No. UM0-2013/08/M/ST2/0025 (LEA-COPIGAL), Grant MNiSW 801/N-COPIN/2010/0 and the Polish Ministry of Science and Higher Education (Grant No. 2011/03/B/ST2/01894).

REFERENCES

[1] C.G.J. Jacobi, *Vorlesungen über Dynamik*; (Ed.) A. Clebsch, printed by G. Reimer, Berlin 1884.

[2] H. Poincaré, *Sur l'équilibre d'une masse fluide animé d'un mouvement de rotation*, *Acta Math.* **7**, 259 (1885).

[3] A. Maj *et al.*, *Nucl. Phys. A* **731**, 319 (2004) and references therein.

[4] A. Maj *et al.*, *Nucl. Phys. A* **687**, 192 (2001).

[5] K. Pomorski, J. Dudek, *Int. J. Mod. Phys. E* **13**, 107 (2004).

[6] A. Maj *et al.*, *Int. J. Mod. Phys. E* **19**, 532 (2010).

[7] K. Mazurek *et al.*, *Acta Phys. Pol. B* **42**, 471 (2011).

[8] F.A. Ivanyuk, K. Pomorski, *Phys. Scr.* **T154**, 014021 (2013).

[9] K. Mazurek, J. Dudek, A. Maj, D. Rouvel, *Phys. Rev. C* **91**, 034301 (2015).

[10] K. Pomorski, J. Dudek, *Phys. Rev. C* **67**, 044316 (2003).

[11] J. Dudek, K. Pomorski, N. Schunck, N. Dubray, *Eur. Phys. J. A* **20**, 165 (2004).